Retinal prosthetic strategy with the capacity to restore normal vision

Sheila Nirenberg[1] and Chethan Pandarinath

Department of Physiology and Biophysics, Weill Medical College of Cornell University, New York, NY 10065

Retinal prosthetics offer hope for patients with retinal degenerative diseases. There are 20–25 million people worldwide who are blind or facing blindness due to these diseases, and they have few treatment options. Drug therapies are able to help a small fraction of the population, but for the vast majority, their best hope is through prosthetic devices [reviewed in Chader et al. (2009) *Prog Brain Res* 175:317–332]. Current prosthetics, however, are still very limited in the vision that they provide: for example, they allow for perception of spots of light and high-contrast edges, but not natural images. Efforts to improve prosthetic capabilities have focused largely on increasing the resolution of the device's stimulators (either electrodes or optogenetic transducers). Here, we show that a second factor is also critical: driving the stimulators with the retina's neural code. Using the mouse as a model system, we generated a prosthetic system that incorporates the code. This dramatically increased the system's capabilities—well beyond what can be achieved just by increasing resolution. Furthermore, the results show, using 9,800 optogenetically stimulated ganglion cell responses, that the combined effect of using the code and high-resolution stimulation is able to bring prosthetic capabilities into the realm of normal image representation.

neural prosthetic | retinal degeneration | vision restoration | neural coding | macular degeneration

Prosthetic devices offer hope for patients with retinal degenerative diseases, such as macular degeneration and retinitis pigmentosa, which affect 20–25 million people worldwide (1–3). These diseases cause a progressive loss of the retina's input cells, the photoreceptors, which leads to severe visual impairment. While the photoreceptors and neighboring tissue degenerate, the retina's output cells remain largely intact. Prosthetic devices make use of this. The approach is to bypass the damaged tissue and provide direct stimulation to the surviving cells, driving them to send visual information to the brain.

While the approach generated a great deal of excitement at its initiation, the devices have not yet achieved the success that was hoped for. Current devices still provide only very limited vision. For example, they allow patients to see spots of light and high-contrast edges, which provide some ability for navigation and gross feature detection, but they are far from providing patients with normal representations of faces, landscapes, etc. (4–6). [With respect to navigation, the devices enable the detection of light sources, such as doorways and lamps, and, with respect to feature detection, they allow discrimination of objects or letters if they span ~7° of visual angle (5); this corresponds to about 20/1,400 vision; for comparison, 20/200 is the acuity-based legal definition of blindness in the United States (7)].

In the past several years, there has been a major push toward improving prosthetic performance. The effort has focused largely on increasing the resolution of the devices' stimulators. The working hypothesis is that the main problem is resolution, and if it were to be increased, prosthetic performance would be substantially boosted. Several groups have been addressing this, using both electrode approaches [high-density, fine-tipped electrode arrays (8, 9)] and optogenetic methods [primarily Channelrhodopsin-2 (ChR2) and its derivatives (10–15)].

However, there is another significant problem, too, and that is how to drive the stimulators to produce normal retinal output.

Briefly, when images enter the retina, they are transformed via retinal processing into patterns of action potentials. The patterns are in a code the brain can read, a code the brain is expecting. Prosthetic devices have not yet incorporated this, raising the possibility that the reason they have not reached their goal is not just because of a resolution problem, but also because of a coding problem (for discussion, see refs. 13, 14, 16–18).

Here we present a prosthetic system that captures this transformation and produces the retina's code; that is, it converts visual input into the same patterns of action potentials that the retina normally produces—and it does this reliably for a broad range of stimuli, including faces, landscapes, animals, people walking, etc. Our results show that incorporation of the code dramatically increases prosthetic performance, well beyond what can be achieved just by increasing resolution. Moreover, they show that the combination of the code and high-resolution stimulation is able to bring prosthetic capabilities up to the level of normal or near-normal image representation.

Results

The prosthetic consists of two parts: an encoder and a transducer (Fig. 1). The encoder mimics the transformations performed by the retina; that is, it converts visual input into the code used by the retina's output cells (the ganglion cells), and the transducer then drives the ganglion cells to fire as the code specifies. Briefly, the encoder is an input/output model of the retina, and the transducer is the light-sensitive protein ChR2 (19, 20); a complete description of the encoder and transducer is given in *SI Materials and Methods*.

As shown in Fig. 1, the steps from visual input to retinal output proceed as follows: Images enter a device that contains the encoder and a stimulator [a modified minidigital light projector (mini-DLP)]. The encoder converts the images into streams of electrical pulses, analogous to the streams of action potentials that would be produced by the normal retina in response to the same images. The electrical pulses are then converted into light pulses (via the mini-DLP) to drive the ChR2, which is expressed in the ganglion cells.

This approach confers on blind retinas the ability to produce normal output, that is, patterns of action potentials that closely match those produced by the normal retina. To show this, we used three sets of recordings. The first set shows normal ganglion cell firing patterns (Fig. 2*A*, *Top*). We presented movies of natural scenes (spatiotemporally varying scenes that include landscapes, faces, people walking, cars, etc.) to the normal mouse retina and recorded ganglion cell responses using a multielectrode array. The responses of several cells, each viewing a different region of the movie, are shown.

A

Encoder — Transducer

e.g., electrodes,
channelrhodopsin-2 (ChR2), etc.

B

Visual input | Encoder | Mini-DLP | Degenerated retina expressing ChR2
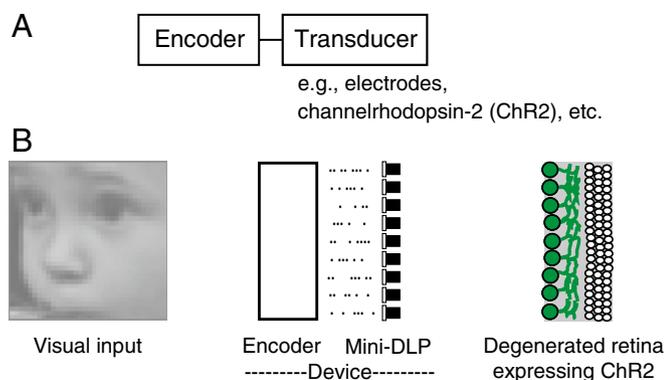--------Device--------

Fig. 1. Schematic of the prosthetic. (*A*) The two components: an encoder and a transducer. The encoder converts the image into the code used by the retinal output cells, the ganglion cells; the transducer drives the ganglion cells to fire spike patterns as the code specifies. As indicated, the transducers can be electrodes, optogenetic stimulators such as ChR2, etc. (*B*) The steps from visual input to retinal output for a blind retina. The input enters a device that contains the encoder and a stimulator (a mini-DLP). The encoder converts the input into patterns of electrical pulses, analogous to the patterns of spikes that would be produced by the normal retina to the same visual input. The patterns of electrical pulses are then converted into patterns of light pulses (via the DLP) to drive the ChR2 in the ganglion cells. For a schematic of the setup as used in the in vitro and in vivo experiments, see Fig. S5.

The second set shows ganglion cell firing patterns from a blind retina when it was presented with the same movies, but this time through the encoder-ChR2 prosthetic (Fig. 2*A*, *Middle*). To obtain blind retinas, we used a standard mouse model of retinal degeneration, the rd1/rd1 mouse line (11, 13, 21, 22). In this line, the degeneration of the outer retina is severe, such that the photoreceptor outer segments are completely lost by 8 wk of age (Fig. 2*C*, *Upper Right*), and, at the physiological level, no visual responses are observed (Fig. 2*E*). To obtain blind retinas that also express ChR2, we bred the rd1/rd1 animals into a mouse line that expresses ChR2 under the regulation of the Thy1 promoter, which is active in retinal ganglion cells (Fig. 2*C*, *Lower Left*); this produced Thy1-ChR2 rd1/rd1 animals. As shown in Fig. 2*C*, *Lower Right*, retinas from these animals show both the severe degeneration of the rd1/rd1 mice (the complete absence of a photoreceptor layer) and the targeted expression of ChR2 in the ganglion cells. Fig. 2*D* shows a whole-mount view of a retina from one of these mice, indicating the dense expression of ChR2 in the ganglion cell population [~33% of ganglion cells express the ChR2 gene (13)].

To present the movies to these retinas through the encoder-ChR2 prosthetic, we proceeded as in Fig. 1: We presented the movies to the encoder/stimulator device, which converted them into streams of electrical pulses and then into streams of light pulses to drive the ChR2. Fig. 2*A*, *Middle*, shows the results: the spike patterns produced by the blind retinas closely match those produced by the normal retinas.

The reason it works is twofold: the encoder (the retinal input/output model) is able to mimic retinal transformations for a broad range of stimuli, including natural scenes, and thus produce normal patterns of pulses (for extensive quantification, see ref. 23), and the transducer (ChR2) has the necessary kinetics/sensitization to follow the encoder's signals. (For longer stretches of data, higher resolution rasters, animated figures, and model performance using primate retina, see Figs. S1, S2, S3, and S4 and Movie S1).

Finally, the last set of recordings shows ganglion cell responses from a blind retina viewing the movies through the standard optogenetic method, where the visual input is presented as is, with no encoding, as in refs. 10–13, 15 (see *Discussion* for a summary of other optogenetic approaches). To set up a fair comparison, we presented the movies using the same stimulator

(same mini-DLP, same wavelength, same peak intensity), so that the only difference between the standard approach and the approach shown in Fig. 2*A*, *Middle*, is the use of the encoder. The results are shown in Fig. 2*A*, *Bottom*: the firing patterns produced by the standard method are clearly different from those produced by the normal retina (compare Fig. 2*A*, *Bottom* and *Top*). Although the standard approach is very effective in producing ganglion cell firing, the firing patterns are not the normal patterns. Fig. 2*B* shows the same series of results as in Fig. 2*A*, but for a second movie, one with different image statistics, to emphasize the reliability of the results.

Fig. 2 *A* and *B* shows that this prosthetic approach allows blind retinas to produce normally coded output. How important is this: what is the potential impact on prosthetic capability? We assessed this using three methods: confusion matrices (Fig. 3), image reconstructions (Fig. 4), and behavioral performance on an optomotor task (Fig. 5).

We first show the results for the confusion matrices (Fig. 3). Briefly, a confusion matrix gives the probability that a neural response to a presented stimulus will be decoded as that stimulus. The vertical axis of the matrix indicates the presented stimulus (i), and the horizontal axis indicates the decoded stimulus (j). The matrix element at position (i,j) gives the probability that stimulus i is decoded as stimulus j. If $j = i$, the stimulus is decoded correctly; otherwise, the stimulus is decoded incorrectly. Put briefly, elements on the diagonal indicate correct decoding; elements off the diagonal indicate confusion.

The top rows of Fig. 3 show the results for ganglion cells from normal retinas, using natural scene stimuli (movies containing faces, landscapes, people walking, etc.). On the left is the performance for individual cells; on the right, for a population of cells. As shown, the individual cells each carry a fair amount of information, and, as a population, they perform very well (nearly all stimuli are identified correctly) (Fig. 3*A*, *Top Right*). The next row shows the results for ganglion cells from blind retinas presented with the same movies, but through the encoder-ChR2 method. The individual cells do not carry quite as much information (there is some scatter across the matrix), but together as a population, they also perform very well (Fig. 3*A*, *Middle*). The last row shows the performance with the standard optogenetic method. The individual cells here carry little information, and even as a population, they are still quite limited (Fig. 3*A*, *Bottom*). Thus, the incorporation of the retina's code, even for a small population of 20 cells, has a very large effect and dramatically boosts prosthetic capabilities. Fig. 3*B* shows the same analysis for a second set of movies (those shown in Fig. 2*B*).

We quantified the performance by calculating the fraction of times that the responses were correctly decoded, averaged over all stimuli. For each matrix, the "fraction correct" is the mean of the values on the diagonal. For the data in Fig. 3 *A* and *B*, the fraction correct for the blind retinas treated with the encoder-ChR2 prosthetic, normalized to the fraction correct for the normal retina, was 96% (Fig. 3*A*) and 81% (Fig. 3*B*). The fraction correct for the blind retinas treated with the standard method, normalized to the fraction correct for the normal retina, was 25% (Fig. 3*A*) and 8% (Fig. 3*B*). On average, the fraction correct for the encoder-ChR2 method was 88% and, for the standard method, 17%.

Next, we performed stimulus reconstructions (Fig. 4). For these experiments we presented an image (of a baby's face) to blind retinas using the two prosthetic systems—the encoder-ChR2 method and the standard optogenetic method—and recorded ganglion cell responses. We then reconstructed the face from the responses using maximum likelihood (25–27), an essentially assumption-free method (*SI Materials and Methods*). To obtain a large enough dataset for the complete reconstruction, we moved the image systematically across the region of the retina from which we were recording, so that responses to all parts of the image could be obtained with a single or small number of retinas. Approximately 9,800 ganglion cell responses were recorded for each image.
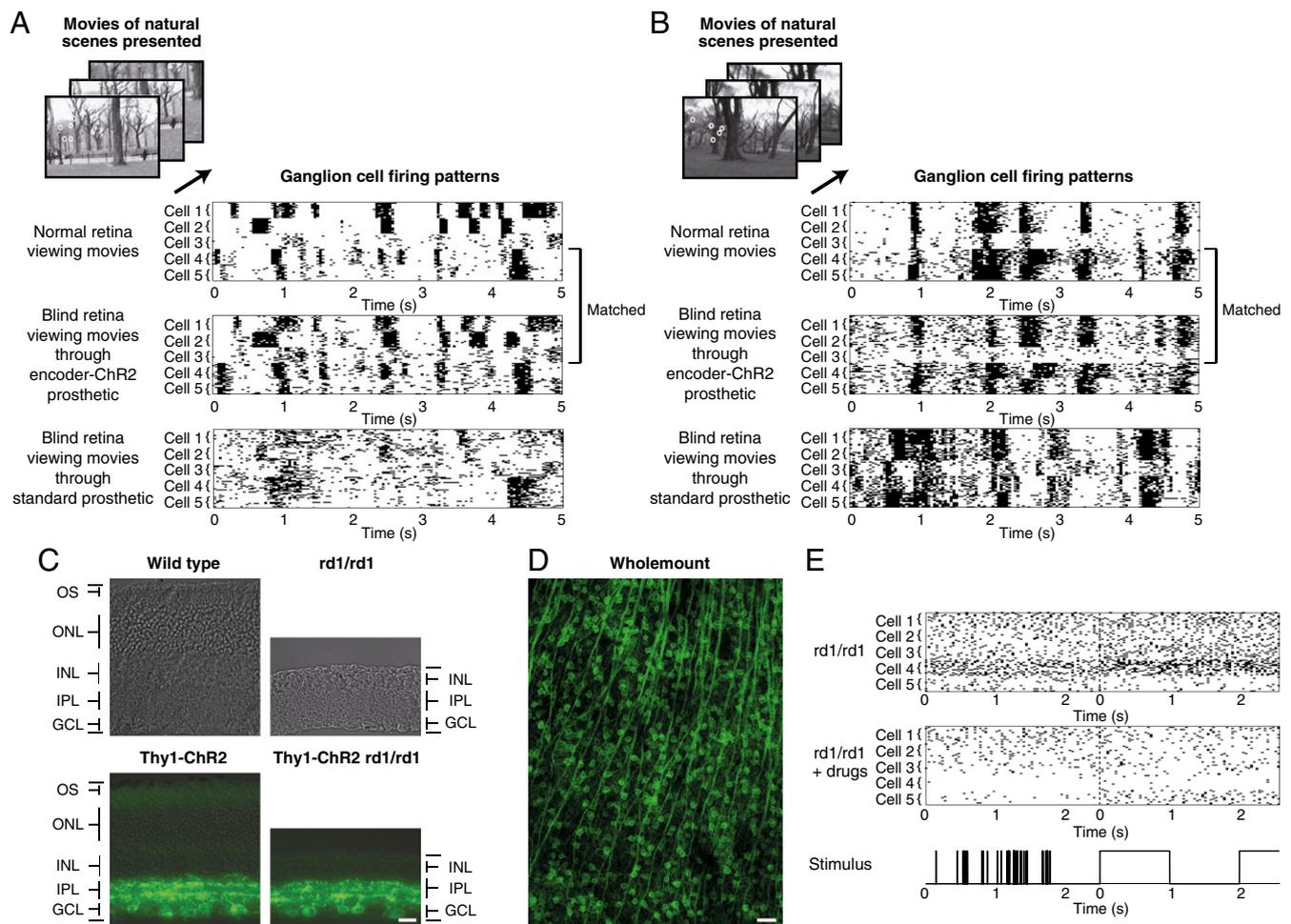
Fig. 2. Blind retinas produce the same output as the normal retina. (*A*) (*Top*) Ganglion cell-firing patterns from a normal, wild-type retina when it was presented with movies of natural scenes (landscapes, faces, people walking, etc). Several cells are shown, including both ON transient and ON sustained cells. (For longer stretches of data, see Figs. S1 and S4.) (*Middle*) Ganglion cell firing patterns from a blind retina (Thy1-ChR2 rd1/rd1 retina) when it was presented with the same movies, but through the encoder-ChR2 prosthetic. As shown, the prosthetic confers on the blind retina the ability to produce firing patterns that closely match those of the normal retina. (*Bottom*) Ganglion cell firing patterns from a blind retina (Thy1-ChR2 rd1/rd1 retina) when it was presented with the same movies, but through the standard optogenetic prosthetic (just ChR2, no encoder). To allow comparison with the middle set of recordings, the movies were presented with the same stimulator (same mini-DLP, same wavelength, same peak intensity), so that the only difference between the *Middle* and *Bottom* recordings was the use of the encoder. As shown, although the standard approach is very effective in driving the ganglion cells, the firing patterns are not the normal patterns. The same receptive field locations were used for all panels to allow comparison of firing patterns (white circles on the movie images). (*B*) Same as in *A*, but using a movie with different image statistics and different ganglion cell types (OFF and ON-OFF types), indicating the robustness of the results. (*C*) Retinal cross sections from wild-type, rd1/rd1, Thy1-ChR2, and Thy1-ChR2 rd1/rd1 mice, respectively. The retina from the Thy1-ChR2 rd1/rd1 animal shows both the severe degeneration characteristic of rd1/rd1 animals (21, 22) (the absence of the photoreceptor layer) and the targeted expression of ChR2 to the ganglion cells. (Scale bar, 20 μm.) (*D*) Whole-mount view of the retina showing the ChR2-expressing cells. (Scale bar, 50 μm.) (*E*) Recordings from rd1/rd1 retinas that do not express ChR2. These retinas were stimulated using the same stimulator as in *A* (same mini-DLP, same wavelength, same peak intensity). (*Top Left*) Ganglion cell responses when the retina was stimulated with the encoded movies. (*Top Right*) Ganglion cell responses when the retina was stimulated with a periodic flash. As shown, and as expected, because these retinas have no photoreceptor outer segments and no ChR2, there is no response to either stimulus, just baseline firing. *Bottom*, *Left and Right*, are same as *Top*, *Left* and *Right*, but with the addition of the neurotransmitter blockers APB, CPP, and NBQX, as in ref. 11; again, no stimulus-dependent responses were observed. For all recordings from degenerated retinas in this paper, i.e., for Figs. 2–4, the retinas were rendered blind using both methods: the use of rd1/rd1 animals and the blockers, the latter included for compulsivity.

Fig. 4*A* shows the original image and Fig. 4*B* shows the image reconstructed from the output of the encoder. Not only is it possible to discern that the image is a baby's face, but also it is possible to tell that it is this particular baby (the baby in Fig. 4*A*), an extremely challenging task. Fig. 4*C* shows the image reconstructed from the responses of the blind retina driven by the encoder-ChR2 method; while there is some loss of information due to passing the code through ChR2, the responses still also produce a close match. Finally, Fig. 4*D* shows the image reconstructed from the responses of a blind retina driven by the standard method. This image is very much degraded with respect to the original. These results, again, indicate that incorporation

of the retina's code into a prosthetic has substantial impact. (Pearson's correlation coefficient between Fig. 4*B* and the original is 0.889; between Fig. 4*C* and the original, 0.760; and between Fig. 4*D* and the original, 0.221.)

Note that the number and density of cells used in Fig. 4 *C* and *D* (~9,800 ganglion cell responses each) correspond to the number and density of cells used in the normal mouse retina (see *SI Materials and Methods* for number of cells per degree of visual angle). Fig. 4*D*, therefore, essentially gives an upper bound on the performance of the standard method (same number and density of cells as the animal uses, with their responses decoded using optimal, i.e., Bayesian, decoding). However, the image shows little
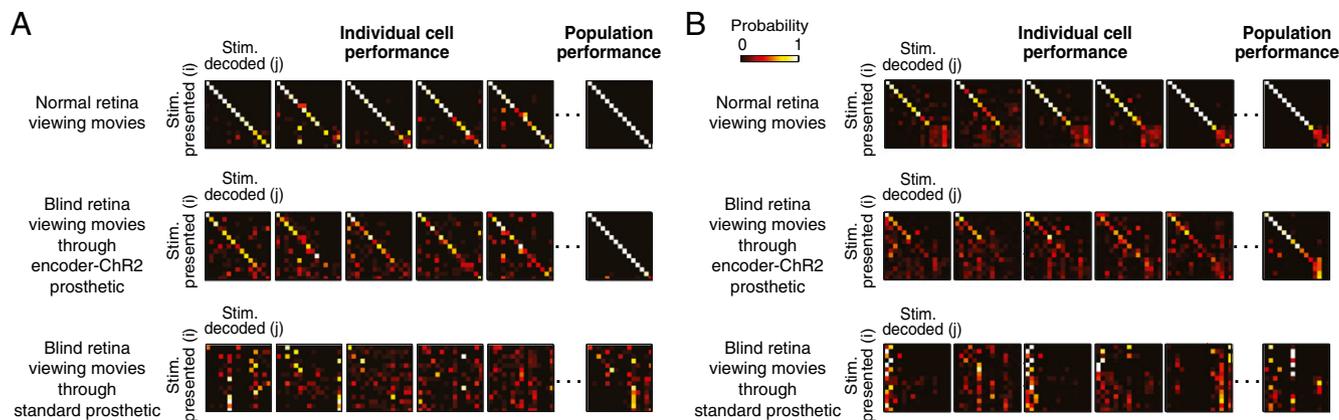
Fig. 3. The output of blind retinas carries the same amount of information, and the same quality of information, as the output of normal retinas, as measured using confusion matrices. (*A*) (Top) Confusion matrices generated from the responses of a normal wild-type retina when presented with movies of natural scenes, which include faces, people walking, landscapes, etc. (*Middle*) Confusion matrices generated from the responses of a blind retina (Thy1-ChR2 rd1/rd1 retina) when it was presented with the same movies, but through the encoder-ChR2 prosthetic. (*Bottom*) Confusion matrices generated from the responses of a blind retina (Thy1-ChR2 rd1/rd1 retina) when it was presented with the same movies, but through the standard optogenetic prosthetic. (*B*) Same as *A*, but for a different set of movies. As shown in both *A* and *B*, the confusion matrices generated from the responses of the blind retinas treated with the encoder-ChR2 prosthetic closely match those of the normal wild-type retinas: the data in the right-most matrices (the population performances) lie along the diagonal line, indicating correct identification of the stimuli. See Fig. S7 for the same analysis performed with an array of bin sizes.

detail. In other words, the results show that the standard approach, which focuses on increasing resolution, has an inherent ceiling on the quality of the image it can produce; even at maximal resolution, image quality is very short of normal. Incorporation of the code breaks through the ceiling.

Finally, we performed a set of behavioral experiments using optomotor tracking. Optomotor behavior was chosen for two reasons: First, it is a reflex and, therefore, does not require behavioral training, which is difficult in animals undergoing retinal degeneration. Second, it requires only a single group of ganglion cells to be targeted: the set of nuclei that controls the optomotor response in the mouse, the accessory optic system, receives input only from ON cells (24, 28), so we can drive the optomotor response with just ON ganglion cell encoders and test the effectiveness of the approach. For these experiments, the animal was head-fixed and placed in front of a liquid crystal display (LCD), which we used to deliver the coded pulses. The LCD was used, rather than the mini-DLP, so that an eye-tracking system could be placed next to the animal's eye. Eye position was tracked using an ISCAN tracking system, which measures infrared reflections off the cornea (*SI Materials and Methods*).

Fig. 5 shows the results. Fig. 5*A* shows the baseline condition for the animal: blind mice show a drift in eye position when no stimulus is present, similar to that observed with blind humans. Fig. 5 *B* and *C* show the results with the standard optogenetic method and the encoder-ChR2 method, respectively. For the standard optogenetic method, the stimulus, a drifting sine wave

grating, was presented as is; for the encoder-ChR2 method, the grating was presented in the encoded form (encoders for transient ON cells were used). As shown in Fig. 5, the encoder-ChR2 method produces tracking, whereas the standard method does not. These results further reveal the importance of incorporating the code: when the image was converted into the code used by the ON ganglion cells, the animal became able to track it.

Discussion

We have developed a unique prosthetic system that consists of two parts: an encoder and a transducer. The encoder converts visual input into the retina's code, that is, the code that the retina normally uses to communicate with the brain. The transducer then drives the retina's output cells, the ganglion cells, to fire as the code specifies.

The system is effective for two reasons. First, the encoder is able to capture the input/output relations of the retina for a broad range of stimuli, including landscapes, faces, animals, people walking, playing, etc.; that is, it produces normal ganglion cell-firing patterns to natural stimuli with great fidelity (as shown here and, additionally, in ref. 23). Second, the transducer (ChR2) has the necessary kinetics to follow the signals the encoder produces.

The effectiveness was shown four ways, starting with the raw data. Fig. 2 shows the firing patterns of the normal retina in response to movies of natural scenes and, below that, the firing patterns produced by the blind retina stimulated via the prosthetic. As shown, the firing patterns produced by the prosthetic

Fig. 4. Images reconstructed from the spike trains of the blind retinas. Although the brain does not necessarily reconstruct images, reconstructions serve as a convenient way to compare methods and give an approximation of the level of visual restoration possible with each approach. (*A*) Original image (a baby's face). (*B*) Image reconstructed from the responses of the encoder. (*C*) Image reconstructed from the responses of the blind retina when it was presented with the face through the

encoder-ChR2 prosthetic. (*D*) Image reconstructed from the responses of the blind retina when it was presented with the face through the standard optogenetic prosthetic. The reconstructions were carried out on a processing cluster in blocks of 10 × 10 or 7 × 7 checks. The decoding was performed using maximum likelihood; that is, for each block, we found the array of gray values that maximized the probability of the observed responses (following ref. 27 for high dimensional searches). The number and density of cells used match that of the normal mouse retina—~9,800 ganglion cell responses per image (see *Materials and Methods* for numbers).
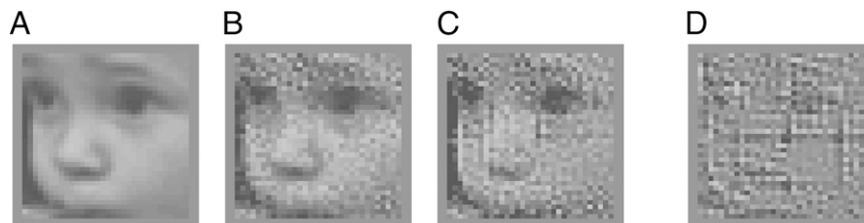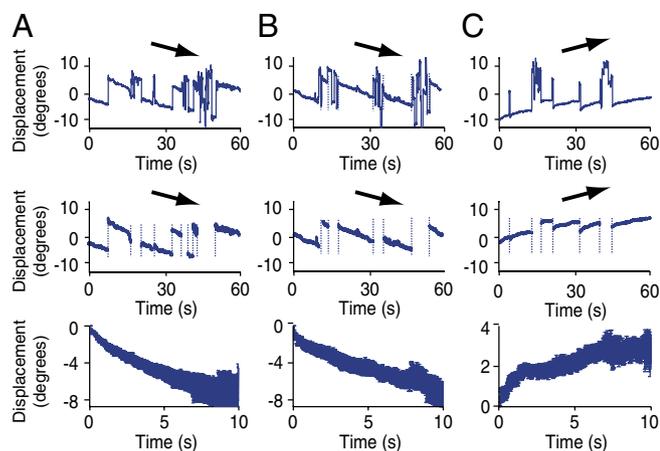
Fig. 5. Behavioral performance: optomotor tracking occurs with the encoder-ChR2 method. (*A*) Baseline condition (no stimulus present). Blind animals show a drift in eye position when no stimulus is present, similar to blind humans; the direction of the drift is downward. (*B*) Response to drifting gratings presented using the standard optogenetic method, that is, where the stimulus was presented unencoded. As shown, no tracking occurs, just the downward drift. (*C*) Response to drifting gratings presented using the encoder-ChR2 method, where the stimulus was presented in its encoded form (i.e., using ON cell encoders; see main text). As shown, when the stimulus was converted into the code used by the ganglion cells, the animal became able to track it. (*A–C, Top*) Representative example of a raw eye-position trace. (*A–C, Middle*) Smooth component (saccades and movement artifacts removed). (*A–C, Bottom*) Average trajectory across all trials (n = 15, 14, and 15 trials, respectively).

closely match those of the normal retina. (For longer stretches of data, higher resolution rasters, and animated figures, see Figs. S1, S2, S3, S4, and Movie S1).

We then quantified the results in Figs. 3–5; that is, we measured the extent to which the firing patterns produced by the prosthetic match those of the normal retina using three independent assays. We first assessed the match using probabilistic (Bayesian) decoding, an essentially assumption-free method. We started by decoding the firing patterns from the normal retina. Briefly, we presented an array of images to the normal retina and recorded the resulting spike trains. We then presented the same images to the blind retina through the prosthetic and again recorded the resulting spike trains. We then asked: would the spike trains from the blind retina be interpreted correctly? If the brain were to receive the spike trains produced by the prosthetic, would it interpret them correctly? This is what the confusion matrices show. Fig. 3 *A* and *B*, *Middle*, shows the fraction of times the spike trains produced by the prosthetic mapped to the same images as the spike trains produced by the normal retina.

We emphasize that we carried this out in a particularly rigorous way: we decoded the spike trains from the prosthetic into the response distributions produced by the normal retina (the likelihoods from the normal retina). This allowed us to explicitly ask: if the brain were *expecting* spike trains from the normal retina, but instead received spike trains from the prosthetic, would it recognize them and map them to the correct image, or would it be confused? What the results showed is that, with high reliability (almost 90% of the time), the brain would map the spike trains from a completely blind retina driven by the prosthetic to the same images as the spike trains from the normal retina.

Fig. 4 also showed probabilistic (Bayesian) decoding, but in the context of a reconstruction task: we reconstructed full grayscale images (faces) on a grid of 35 × 32 pixels, which is a very high dimensional problem, especially with uniform (i.e., uninformative) priors. For these experiments, we used several thousand ganglion cell responses, the same number of cells that the animal would use (see *Materials and Methods* for cell

numbers). Similar to the results shown in Fig. 3, these results showed that the spike trains produced by the prosthetic were highly reliable: the baby's face was faithfully reconstructed—to the extent that it could be recognized as the same face as the original.

In addition to showing the reconstruction from the blind retina, we also showed a reconstruction from the pulses produced by the encoder. This demonstrated the effectiveness of the two parts of the prosthetic separately. The reconstruction from the pulses of the encoder shows how well we captured the code, and the reconstruction from the blind retina shows how well ChR2 follows the encoder. As shown, although there is some information lost as the code passes through ChR2, it is relatively small (compare Fig. 4 *B* and *C*).

Finally, we tested the efficacy of the prosthetic at the level of behavior (Fig. 5). We chose an optomotor tracking task because it does not require training (which is difficult in animals with retinal degeneration), and, because it can be driven by a single group of ganglion cells, the ON cells, we were able to drive the response with just ON cell encoders and assess the effectiveness of the approach. The results showed that the prosthetic makes tracking possible: when the stimulus, a drifting grating, was presented through the encoder, it became detectable to the animal, and tracking ensued. This emphasizes, at the level of an in vivo experiment, that the encoder component is critical; without it, tracking responses are random.

In sum, the raw data (Fig. 2) and the three functional assays (Figs. 3–5) provide very strong evidence that we have the essential building blocks for building a highly effective retinal prosthetic.

Comparison with Other Optogenetic Approaches. As mentioned in the Introduction, other groups have used optogenetic approaches to drive the degenerated retina. The main strategy has been to drive the treated retina directly with the visual stimulus, intensified to a level that could drive ChR2. The target cells were initially ganglion cells (10, 12, 13), and, later, bipolar cells (11, 15). These were major pioneering studies, showing that blind retinas could become responsive to light using ChR2. However, there was still the issue of processing, of driving the retina to produce normal responses. This was one of the main reasons for shifting from ganglion cells to bipolar cells (11): because bipolar cells are closer to the retina's normal input cells, shifting to them would allow some aspects of normal processing to be preserved. However, the retinal output was not normal, even for simple stimuli, such as flashes (11, 15). Presumably, this is because optogenetic stimulation at the level of the bipolar cell still bypasses too much significant circuitry, such as circuitry that contributes to temporal processing, center/surround antagonism, and possibly other operations.

Recently, Greenberg et al. (14) focused on center/surround antagonism using a clever optogenetic strategy. They created an excitatory center and an inhibitory surround at the level of the ganglion cell using antagonistic opsins. Specifically, they directed ChR2 to the soma and halorhodopsin to the dendrites using specific gene regulatory elements. This approach by itself did not create center/surround with normal spatial characteristics, but they were able to remedy this with a preprocessing step of Gaussian blur. Still, as the authors themselves state, this constituted only a first step toward building retinal processing; that is, it creates center/surround, but other aspects of the processing have not yet been captured.

Our approach is different: instead of trying to recreate computations in the retina, i.e., in the actual tissue, we carry them out in an external device. This has two key advantages. First, one can develop a more complete model of retinal computations without the additional constraint of having to find molecular components to implement them. Second, because we are not using ChR2 as a computing mechanism, we are making much smaller demands on what it needs to achieve. We use ChR2 only as a transducer, a means to transfer the output of the computational model to the nervous system, not as a computing device itself. These advantages also allow the approach to generalize to other prosthetics

problems (or other brain/machine interface applications). The strategy can be applied to any system in which the computations can be mathematically characterized. This allows problems to be solved on a much faster timescale.

Potential for Translation. For delivery of channelrhodopsin, several groups, including ourselves, are using adeno-associated viral (AAV) vectors, as clinical and preclinical trials have shown both safe and efficient gene delivery with AAV in ocular settings (29–33). In terms of driving the channelrhodopsin, the mini-DLP, because it is small, can be readily incorporated into an eyeglasses-based device (Figs. S5 and S6).

One potential bottleneck for the development of this prosthetic system for patients is the issue of targeting codes to specific ganglion cell classes. The ganglion cell population contains several cell classes. This might raise the concern that, to produce quality vision, one would need to stimulate each class with its appropriate code. However, strong evidence suggests that this is not the case. Patients with Duchenne's muscular dystrophy lack ON channel transmission, and, thus, see exclusively through OFF cells (34, 35). These patients do not report vision problems (34, 35). They are actually unaware of the deficiency; it becomes apparent only through electrophysiological measures (35). Thus, driving just OFF cells with their code has the potential to produce substantial vision restoration [see *SI Materials and Methods* for encoder performance for specific ganglion cell types: for mouse (Fig. S1) and for primate (Fig. S4), including ON and OFF midget and parasol classes (Fig. S4)].

Thus, although it is likely that there will be many hurdles to overcome to bring this technology to patients, the major ones—a vector (AAV) for delivering ChR2 to ganglion cells, an encoder/stimulator device to drive them, and the fact that targeting a single ganglion cell class by itself can bring substantial vision restoration—have already been addressed, substantially increasing the probability of success.

Importance of Retinal Coding in Light of Limited Plasticity. Recent studies have shown that front-end processing in the visual system is much less plastic than that in auditory and somatosensory systems (summarized in ref. 36). This has been shown in animals and also in adult patients with macular degeneration (36, 37). The lower plasticity may explain why standard retinal prosthetics have been less successful than cochlear implants. The limited plasticity puts a much heavier burden on retinal prosthetics to produce signals close to those of the normal retina.

In sum, our results show that incorporating the code dramatically increases prosthetic capabilities. Although increasing resolution also improves performance, there is an inherent ceiling on the quality of image this can produce; adding the code breaks through this barrier. The coded output combined with high-resolution stimulation makes natural vision restoration possible.

Materials and Methods

A complete description of materials and methods, including a description of the model, the device, the animals, and the analysis methods, is provided in *SI Materials and Methods*.

1. Chopdar A, Chakravarthy U, Verma D (2003) Age related macular degeneration. *BMJ* 326:485–488.
2. Resnikoff S, Pascolini D, Mariotti SP, Pokharel GP (2008) in *Bull World Health Organ* 86(1):63–70.
3. Gordois A, Pezzullo L, Cutler H (2010) *The Global Economic Cost of Visual Impairment* (Access Economics Pty Limited, Canberra, Australia).
4. Chader GJ, Weiland J, Humayun MS (2009) Artificial vision: Needs, functioning, and testing of a retinal electronic prosthesis. *Prog Brain Res* 175:317–332.
5. Zrenner E, et al. (2009) Subretinal microelectrode arrays allow blind retinitis pigmentosa patients to recognize letters and combine them to words. *Proc 2nd Int Conf IEEE Biomed Eng Inf*, pp 1–4.
6. Winter JO, Cogan SF, Rizzo, JF, III (2007) Retinal prostheses: Current challenges and future outlook. *J Biomater Sci Polym Ed* 18:1031–1055.
7. Congdon N, et al.; Eye Diseases Prevalence Research Group (2004) Causes and prevalence of visual impairment among adults in the United States. *Arch Ophthalmol* 122: 477–485.
8. Loudin JD, et al. (2007) Optoelectronic retinal prosthesis: System design and performance. *J Neural Eng* 4:S72–S84.
9. Sekirnjak C, et al. (2008) High-resolution electrical stimulation of primate retina for epiretinal implant design. *J Neurosci* 28:4446–4456.
10. Bi A, et al. (2006) Ectopic expression of a microbial-type rhodopsin restores visual responses in mice with photoreceptor degeneration. *Neuron* 50(1):23–33.
11. Lagali PS, et al. (2008) Light-activated channels targeted to ON bipolar cells restore visual function in retinal degeneration. *Nat Neurosci* 11:667–675.
12. Tomita H, et al. (2009) Visual properties of transgenic rats harboring the channelrhodopsin-2 gene regulated by the thy-1.2 promoter. *PLoS ONE* 4:e7679.
13. Thyagarajan S, et al. (2010) Visual function in mice with photoreceptor degeneration and transgenic expression of channelrhodopsin 2 in ganglion cells. *J Neurosci* 30: 8745–8758.
14. Greenberg KP, Pham A, Werblin FS (2011) Differential targeting of optical neuromodulators to ganglion cell soma and dendrites allows dynamic control of center-surround antagonism. *Neuron* 69:713–720.
15. Doroudchi MM, et al. (2011) Virally delivered channelrhodopsin-2 safely and effectively restores visual function in multiple mouse models of blindness. *Mol Ther* 19: 1220–1229.
16. Eckmiller R, Neumann D, Baruth O (2005) Tunable retina encoders for retina implants: why and how. *J Neural Eng* 2:S91–S104.
17. Nirenberg S (2011) Strategies for finding neural codes. *Visual Population Codes*, eds Kriegeskorte N, Kreiman G (MIT Press, Cambridge, MA).
18. Jacobs AL, et al. (2009) Ruling out and ruling in neural codes. *Proc Natl Acad Sci USA* 106:5936–5941.
19. Nagel G, et al. (2003) Channelrhodopsin-2, a directly light-gated cation-selective membrane channel. *Proc Natl Acad Sci USA* 100:13940–13945.
20. Boyden ES, Zhang F, Bamberg E, Nagel G, Deisseroth K (2005) Millisecond-timescale, genetically targeted optical control of neural activity. *Nat Neurosci* 8:1263–1268.
21. Grimm C, et al. (2004) Constitutive overexpression of human erythropoietin protects the mouse retina against induced but not inherited retinal degeneration. *J Neurosci* 24:5651–5658.
22. Hackam AS, et al. (2004) Identification of gene expression changes associated with the progression of retinal degeneration in the rd1 mouse. *Invest Ophthalmol Vis Sci* 45:2929–2942.
23. Nirenberg S, Pandarinath C, Ohiohenuan I (2011) Retina prosthesis. International Patent WO2011106783.
24. Dann JF, Buhl EH (1987) Retinal ganglion cells projecting to the accessory optic system in the rat. *J Comp Neurol* 262(1):141–158.
25. Quian Quiroga R, Panzeri S (2009) Extracting information from neuronal populations: Information theory and decoding approaches. *Nat Rev Neurosci* 10(3):173–185.
26. Kass RE, Ventura V, Brown EN (2005) Statistical issues in the analysis of neuronal data. *J Neurophysiol* 94:8–25.
27. Paninski L, Pillow J, Lewi J (2007) Statistical models for neural encoding, decoding, and optimal stimulus design. *Prog Brain Res* 165:493–507.
28. Giolli RA, Blanks RHI, Lui F (2006) The accessory optic system: Basic organization with an update on connectivity, neurochemistry, and function. *Prog Brain Res* 151:407–440.
29. Maguire AM, et al. (2008) Safety and efficacy of gene transfer for Leber's congenital amaurosis. *N Engl J Med* 358:2240–2248.
30. Hauswirth WW, et al. (2008) Treatment of leber congenital amaurosis due to RPE65 mutations by ocular subretinal injection of adeno-associated virus gene vector: short-term results of a phase I trial. *Hum Gene Ther* 19:979–990.
31. Cideciyan AV, et al. (2009) Vision 1 year after gene therapy for Leber's congenital amaurosis. *N Engl J Med* 361:725–727.
32. Simonelli F, et al. (2010) Gene therapy for Leber's congenital amaurosis is safe and effective through 1.5 years after vector administration. *Mol Ther* 18:643–650.
33. Mancuso K, et al. (2009) Gene therapy for red-green colour blindness in adult primates. *Nature* 461:784–787.
34. Fitzgerald KM, Cibis GW, Giambrone SA, Harris DJ (1994) Retinal signal transmission in Duchenne muscular dystrophy: Evidence for dysfunction in the photoreceptor/depolarizing bipolar cell pathway. *J Clin Invest* 93:2425–2430.
35. Cibis GW, Fitzgerald KM (2001) The negative ERG is not synonymous with night-blindness. *Trans Am Ophthalmol Soc* 99:171–175, discussion 175–176.
36. Fine I (2008) The effects of visual deprivation. *Artificial Sight*, eds Humayun MS, Weiland JD, Chader G, Greenbaum E (Springer, New York), pp 47–70.
37. Baseler HA, et al. (2011) Large-scale remapping of visual cortex is absent in adult humans with macular degeneration. *Nat Neurosci* 14:649–655.

NEUROSCIENCE